

- Jacobus, W. J., & Lehninger, A. L. (1973) *J. Biol. Chem.* 248, 4803-4810.
- Katzenellenbogen, B. S., & Gorski, J. (1972) *J. Biol. Chem.* 247, 1299-1305.
- Katzenellenbogen, B. S., & Gorski, J. (1975) in *Biochemical Actions of Hormones* (Litwak, G., Ed.) Vol. 3, pp 187-243, Academic Press, New York.
- Kaye, A. M., Sheratzky, D., & Lindner, H. R. (1972) *Biochim. Biophys. Acta* 261, 475-486.
- Lawson, J. W., & Veech, R. L. (1979) *J. Biol. Chem.* 254, 6528-6537.
- Mairesse, N., & Galand, P. (1982) *Mol. Cell. Endocrinol.* 28, 671-679.
- Martell, A. E., & Schwarzenbach, G. (1956) *Helv. Chim. Acta* 39, 653-661.
- Meyer, R. A., Kushmerick, M. J., & Brown, T. R. (1982) *Am. J. Physiol.* 242, C1-C11.
- Nanninga, L. B. (1961a) *Biochim. Biophys. Acta* 54, 330-338.
- Nanninga, L. B. (1961b) *Biochim. Biophys. Acta* 54, 338-344.
- Noda, L., Kuby, S. A., & Lardy, H. A. (1954) *J. Biol. Chem.* 210, 83-95.
- Notides, A., & Gorski, J. (1966) *Proc. Natl. Acad. Sci. U.S.A.* 56, 230-235.
- Oliver, J. M., & Kellie, A. E. (1970) *Biochem. J.* 119, 187-191.
- Reiss, N., & Kaye, A. M. (1981) *J. Biol. Chem.* 256, 5741-5749.
- Rosen, J. M., & O'Malley, B. W. (1975) in *Biochemical Actions of Hormones* (Litwak, G., Ed.) Vol. 3, pp 271-315, Academic Press, New York.
- Schoubridge, E. A., Briggs, R. W., & Radda, G. K. (1982) *FEBS Lett.* 140, 288-292.
- Shulman, R. G., Brown, T. R., Ugurbil, K., Ogawa, S., Cohen, S. M., & den Hollander, J. A. (1979) *Science (Washington, D.C.)* 205, 160-166.
- Smith, D. E., & Gorski, J. (1968) *J. Biol. Chem.* 243, 4169-4174.
- Spooner, P. J., & Gorski, J. (1972) *Endocrinology (Philadelphia)* 91, 1273-1284.
- Veech, R. L., Lawson, W. R., Cornell, N. W., & Krebs, H. A. (1979) *J. Biol. Chem.* 254, 6538-6547.
- Volfin, P., Clauser, H., Gautheron, D., & Eboue, D. (1961) *Bull. Soc. Chim. Biol.* 43, 107-119.
- Walaas, O. (1950) *Acta Physiol. Scand.* 21, 27-33.
- Walaas, O., & Walaas, E. (1950) *Acta Physiol. Scand.* 21, 1-17.
- Walker, M. D., & Kaye, A. M. (1981) *J. Biol. Chem.* 256, 23-26.
- Wu, S. T., Pieper, G. M., Salhany, J. M., & Eliot, R. S. (1981) *Biochemistry* 20, 7399-7403.

## Internal and External Alkali Ion Complexes of Enniatin B: An Empirical Force Field Analysis<sup>†</sup>

Shneior Lifson,\* Clifford E. Felder, and Abraham Shanzer

**ABSTRACT:** The empirical force field method is used to calculate conformations and energies of the natural ion carrier enniatin B (EnB) and its alkali ion complexes. Solvent effects are circumvented by focusing the study on conformational characteristics and trends in ionophoric behavior, which do not require an evaluation of solvent interactions. A few calculated, low-energy conformations of the EnB ring are presented. The  $C_3$ -symmetric conformation of EnB is analyzed in detail. Its rotational isomeric states of the isopropyl side chains are found to interact strongly with its carbonyl and *N*-methyl groups, thus restricting significantly the flexibility of EnB's skeletal ring. Two kinds of 1:1 EnB-ion complexes are obtained: internal and external. In internal complexes, the ion is located at or near the center of an octahedral cavity formed by the six carbonyls of EnB and binds to all these carbonyls. The large strain energy imposed on the ligand by bending the carbonyls inward destabilizes the internal binding.

In external complexes, the ion binds only to the three carbonyls of the hydroxyisovaleryl residues, but its binding energy can be the same or even stronger, due to the better dipole-ion alignment and lower strain energy.  $Li^+$  is a poor binder, in that it binds only internally and is too small to bind simultaneously to all six carbonyls.  $Na^+$  fits the molecular cavity well and is the best internal binder. It can also form stable external complexes and is expected to prefer such complexes in polar solvents, where it is partly solvated.  $K^+$  is too big for the EnB cavity, but it squeezes in asymmetrically by distorting the molecule.  $Rb^+$  can hardly fit internally and  $Cs^+$  not at all. However, these three ions do bind quite well externally. External 1:1 EnB-ion complexes can bind a second EnB ligand to form sandwich 2:1 dimer complexes. The calculated energy of the second ligand binding is stronger than the 1:1 external complex energy for  $K^+$ ,  $Rb^+$ , and  $Cs^+$  but not for  $Na^+$ , implying that the 2:1 complex is more favored by the larger ions.

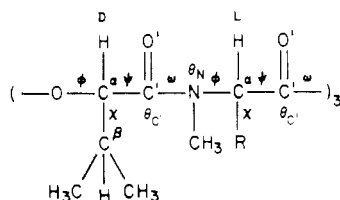
**E**nniatis are natural ion carriers whose biological functions are determined by their ability to transport cations across lipid bilayer membranes. Enniatis, and particularly enniatin B,<sup>1</sup>

have been studied extensively and reviewed comprehensively (Ovchinnikov et al., 1974; Burgermeister & Winkler-Oswatitsch, 1977; Ovchinnikov & Ivanov, 1982). They are cyclic depsipeptides, composed of alternating D-hydroxyisovaleric acid

<sup>†</sup> From the Departments of Chemical Physics (S.L. and C.E.F.) and Organic Chemistry (A.S.), Weizmann Institute of Science, 76100 Rehovot, Israel. Received October 11, 1983. This research was partly supported by the Minerva Foundation, Munich, West Germany, and by the U.S.-Israel Binational Science Foundation, Jerusalem, Israel.

<sup>1</sup> Abbreviations: EnB, enniatin B; (LacAla)<sub>3</sub>, EnB methyl side chain analogue [(D-lactyl-L-N-methylalanyl)<sub>3</sub>]; Lac<sub>6</sub>, EnB hexalactyl analogue [(D-lactyl-L-lactyl)<sub>3</sub>].

(D-HyIV) and *N*-methyl L-amino acid residues, linked by amide and ester bonds, according to the general formula:



where D and L denote the chirality of  $C^\alpha$ ,  $\phi$ ,  $\psi$ ,  $\omega$ , and  $\chi$  denote the torsion angles of the corresponding bonds, and  $\theta_C$  and  $\theta_N$  denote out-of-plane torsional angles. In enniatin B (EnB), the amino acid component is L-*N*-methylvaline (L-NMVal), so that both HyIV and NMVal have the same isopropyl side chain, while in other enniatins the amino acid component is another *N*-methylated hydrophobic amino acid such as isoleucine, leucine, or phenylalanine.

EnB binds alkali ions, generally in a 1:1 ratio, with stability constants that vary with ion species and solvent, as well as with the concentrations of both the ligand and the ion. In alcohols (EtOH and MeOH), the stability constants are highest for  $K^+$ , followed by slightly lower values for  $Rb^+$ ,  $Cs^+$ , and  $Na^+$  and much lower for  $Li^+$  [see Table 7 of Burgermeister & Winkler-Oswatitsch (1977)]. At sufficiently high ligand concentrations, high ligand to ion ratios, and appropriately chosen solvents, there is evidence from nuclear magnetic resonance (NMR) and circular dichroism (CD) titrations for 2:1 EnB:cation binding ratios (Ivanov et al., 1973), with stability constants in the order  $K^+ > Cs^+ \gg Na^+$  (Gurevich, 1980). Studies of conductance through lipid bilayer membranes indicate a complexation stoichiometry of 3:2 for  $Cs^+$ , 2:1 for  $K^+$ , and 1:1 for  $Na^+$  at an enniatin B concentration range of  $10^{-7} \sim 10^{-5}$  mol/L.

The 1:1 stoichiometry has been attributed (Ovchinnikov et al., 1974) to the binding of the cation inside the ring cavity by the six carbonyls, while higher stoichiometries were attributed to sandwiching the cation between adjacent rings. It has been suggested (Ovchinnikov et al., 1974) that enniatin possesses a symmetric cage-like conformation when it forms ion complexes or when it is dissolved in polar solvents, where the mutual repulsions between the carbonyls are screened by the solvent, while in nonpolar solvents of low dielectric constants enniatin B attains a more stable asymmetric conformation. It has been further suggested (Ovchinnikov et al., 1974) that the low binding selectivity of the enniatins for different alkali ions is due to the flexibility of the ring in its symmetric cage-like conformation.

The search for allowed conformations of enniatin led to a theoretical prediction of a number of such conformations (Popov et al., 1970), on the basis of an examination of the allowed energy minima of the residues forming the ring. Subsequent publications, in part resting on  $^1H$  NMR of EnB in polar and nonpolar solvents, contain a modified set of conformations (Ovchinnikov et al., 1974). The molecular conformation in the crystalline state was determined by single crystal diffraction of free EnB (Tischenko et al., 1976) and of its  $K^+$  cavity-bound complex (Dobler et al., 1969).

This short and incomplete review of the available literature on EnB may be summarized by viewing this molecule as being asymmetric in nonpolar solvents and  $C_3$  symmetric in polar media or when complexed. It is sufficiently flexible to accommodate the alkali ions  $Na^+$  to  $Cs^+$  in its internal cavity as 1:1 complexes and is also capable of forming 2:1 sandwich complexes under favorable conditions. The results of our calculations are in reasonable agreement with the findings of

the extensive experimental studies of enniatin B and its ion complexes. They indicate, however, that nontrivial modifications and extensions of the interpretation of the observed facts are necessary. These modifications improve, we believe, the general view of EnB and its mode of functioning as an ion carrier.

We find that the flexibility of the enniatin molecule is rather limited, in spite of the almost free rotation of the  $\phi$  and  $\psi$  torsional angles. Not only are the bonds and bond angles quite rigid but also so are the out-of-plane angles  $\theta_C$  and  $\theta_N$ , as well as the torsional angles  $\omega$  around amide and ester bonds, due to their partial double bond character. The rotational freedom is also limited by the condition of ring closure. Therefore, the ring exhibits flexibility only for some selected directions of motion, and even these are hindered by the interaction of the isopropyl side chains with the carbonyls and *N*-methyls of the EnB ring. These limitations in the conformational space of enniatin also limit the number of equilibrium conformations. The  $C_3$ -symmetric conformation is calculated to be one of the most stable conformations even in vacuum (or in nonpolar solvents), in spite of the repulsions between the carbonyls, since pushing two carbonyls apart moves them nearer to other carbonyls. As a consequence of the limited flexibility of EnB and the fit of its cavity to the size of  $Na^+$ , only this ion binds comfortably in the cavity. The 1:1 EnB complexes of  $K^+$ ,  $Rb^+$ , and  $Cs^+$  are most likely external, and so is probably that of  $Na^+$  in protic solvents like alcohols. The same considerations of limited flexibility and cavity size also explain why  $Na^+$  forms 1:1 complexes, while  $K^+$  forms 2:1 complexes in transport through purely nonpolar lipid membranes.

## Theory

**Theoretical Considerations.** The present theoretical analysis of the energies and conformations of EnB and its alkali cation complexes is based on the application of a carefully chosen empirical force field. The empirical force field method has been advanced during the last decade to yield consistently accurate predictions of many molecular properties such as intramolecular strain energies, crystalline structures and packing energies, molecular conformations, vibrational spectra, dipole moments, etc. [see Lifson (1983)]. Recently, we applied the method to design the synthesis of new ion carrier molecules, on the basis of predicting their ionophoric characteristics (Shanzer et al., 1983; Lifson et al., 1983; Felder et al., 1983). Some of the considerations and results included in these papers are relevant to our present study and will be reviewed briefly.

The most striking property of ionophoric behavior is the delicate balance between several factors, some of them originating from very strong interactions. On the one hand, the selectivity of  $K^+$  vs.  $Na^+$  binding, or the balance between monomer (1:1) binding vs. dimer (2:1) binding, depends on small free-energy differences,  $\Delta G$ , according to the Boltzmann distribution  $\exp[-\Delta G/(RT)]$ . (At room temperature  $RT$  is 0.6 kcal/mol; thus free-energy differences of 2–3 kcal/mol yield binding ratios of 28–150). On the other hand, the enthalpies of hydration of  $Li^+$ ,  $Na^+$ ,  $K^+$ ,  $Rb^+$ , and  $Cs^+$  are very large: -130, -104, -83, -78, and -70 kcal/mol, respectively (Noyes 1962). Thus, the interaction between the ionophore and the complexed ion must be of the same order, for binding to take place.

The main interactions comprise, first and foremost, the Coulomb interaction between the ion and the atomic partial charges of the ionophore, particularly the carbonyls, accompanied by the polarization interaction between the ion and the ionophore, which also amounts to several tens of kilocalories per mol (Lifson et al., 1983); then there is the strain energy

Table I: Symmetric Conformations of Enniatin B and Its Methyl Side Chain Analogues (deg)

compd	hydroxy residue				amino residue				
	$\phi$	$\psi$	$\theta_{C'}$	$\omega$	$\theta_N$	$\phi$	$\psi$	$\theta_{C'}$	$\omega$
EnB (cryst) <sup>a</sup>	108 ± 3	-126 ± 1	13 ± 1	176 ± 4	-14 ± 2	-109 ± 4	128 ± 4	19 ± 5	179 ± 9
EnB (calcd)	112	-98	0	-178	1	-127	112	3	178
(LacAla) <sub>3</sub> (calcd 1)	116	-89	0	180	0	-137	109	-1	-178
(LacAla) <sub>3</sub> (calcd 2) <sup>b</sup>	74	-136		(180)		-103	171		(180)

<sup>a</sup> Tishchenko et al. (1976). The ± indicates the range of variation due to deviations from C<sub>3</sub> symmetry. <sup>b</sup> Ovchinnikov et al. (1974).

accompanying the conformational changes imposed by the ion on the ionophore upon complexation; and finally, there is the free-energy difference between the solvation of the complexed and the free ionophore. A detailed evaluation of all these interactions in the degree of accuracy necessary to obtain the free-energy balance of the complexation reaction within experimental accuracy would be next to an impossible task. However, it is possible to single out some of the major factors and consider them in some detail, such that relevant questions can be asked and definite answers may be obtained with the help of a reliable force field.

The questions we ask are all related to the equilibrium conformations of the ligand and the complex and the electrostatic and strain energies involved. Thus, the strength of the Coulomb interaction between the ion and its ligand, the degree of conformational deformation following ligation and the accompanying strain energy, the symmetry of the ionophoric cavity and its distortion when the ion is either too large or too small for the cavity, and the comparison between alternative modes of binding all vary from ion to ion in a way that yields a detailed picture of the ionophoric phenomenon.

As is to be expected, such theoretical analysis is by its very nature approximate, and not always will it represent reality with sufficient reliability. Nevertheless, it gives a better insight into the behavior of the ion carrier and its ion complexes than that available at present and offers new alternatives for the interpretation of available experimental data. At the same time, it puts to test the power and limitations of the empirical force field method and may perhaps lead the way to its improvement as a theoretical tool in chemistry and molecular biology.

**Computations.** The empirical force field is the same as in our preceding paper (Lifson et al., 1983), except that it contains in addition the appropriate energy functions for the amide group and for the heavier ions Rb<sup>+</sup> and Cs<sup>+</sup>. It represents the energy of the molecule and its ion complexes as a function of all internal coordinates and interatomic distances of nonbonded atoms. Equilibrium conformations are obtained by minimizing the total energy.

The amide intramolecular parameters were taken from the same source as the ester group parameters (Hagler et al., 1979), where they had been optimized to fit both conformational and vibrational data on *N*-methylacetamide, and the amide nonbonded parameters were taken from Lifson et al. (1979). The CH<sub>3</sub> group was replaced by an "extended atom" (M. Levitt and S. Lifson, unpublished results). The Lennard-Jones potential parameters  $r^*$  and  $\epsilon$  for Rb<sup>+</sup> and Cs<sup>+</sup> were derived in the same way as previously for Li<sup>+</sup>, Na<sup>+</sup>, and K<sup>+</sup> and from the same sources (Ketelaar, 1953; Buckingham, 1937). The values of  $r^*$  and  $\epsilon$  for all alkali ions and the CH<sub>3</sub> extended atom are, in angstroms and kilocalories per mol e, as follows: Li<sup>+</sup>, 2.58, 0.00156; Na<sup>+</sup>, 3.20, 0.0165; K<sup>+</sup>, 3.84, 0.0498; Rb<sup>+</sup>, 3.96, 0.0877; Cs<sup>+</sup>, 4.36, 0.1083; CH<sub>3</sub>, 4.17, 0.092.

Stereoviews of the calculated conformations of EnB and its ion complexes [produced by the computer code PLUTO of Motherwell (1979)] are introduced in order to visualize the

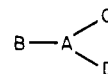
results and facilitate the discussion. The atoms in the stereoviews are scaled at 25% of the atomic contact radii, to leave the view of the molecule open. The coordinate system is always fixed along the three axes of inertia, with the Z axis as the axis of symmetry (or more generally as the largest inertial axis). The stereoviews are mostly accompanied by two perpendicular projections of the asymmetric repeating unit of the molecule along the Z and the Y axes, scaled in half-angstrom units. Atomic contact radii are scaled down further, so that the Cartesian coordinates of all atoms can be read off from these projections to a reasonable accuracy. Such a presentation encompasses in a nutshell the computer output of molecular conformations and may serve to calculate easily any geometric property not included in the tables, e.g., interatomic contact distances.

## Results and Discussion

The following notation is used throughout this section. The distance between an ion and a carbonyl oxygen is denoted by  $r_0$ . The distance between carbonyl oxygens belonging to nearest-neighbor residues and residing on opposite sides of the ring plane is denoted by  $r_1$ . The distance between carbonyl oxygens belonging to next nearest neighbors and residing on the same side of the ring plane is denoted by  $r_2$ . The angle between the ion-oxygen "bond" vector (Z<sup>+</sup>-O') and the oxygen-carbon bond vector (O'=C') is defined as  $\alpha$  (zero when they are collinear).

**(I) Equilibrium Conformations of EnB and Their Relative Strain Energies.** (a) *Symmetric Ring Conformation.* EnB possesses a number of equilibrium conformations. Among them, the one with a 3-fold (C<sub>3</sub>) symmetry is of particular interest, since it is closely related to the conformations of the ion-EnB complexes. In Table I, the conformation in the crystalline state, as derived from X-ray diffraction (Tishchenko et al., 1976), and several calculated symmetric conformations of EnB and (LacAla)<sub>3</sub> are presented and compared.

In the crystal, the C<sub>3</sub> molecular symmetry is imperfect, and the first row of Table I gives the average torsional angles of the ring and their span of variation. It contains also the out-of-plane angles  $\theta_{C'}$  and  $\theta_N$  around the ring atoms C' and N, respectively. (An out-of-plane angle  $\theta_A$  for a structure



is the angle between the plane through the atoms ABC and the plane through the atoms ADB; it is zero when all four atoms are coplanar). The isopropyl side chains are all in the equatorial trans rotoisomeric state (see Figure 1), whose calculated energy is the lowest among all rotoisomeric states (see below).

The second row in Table I contains the corresponding calculated conformational variables for the same equatorial state of the side chains. Since it was derived by a search technique (Lifson et al., 1983) with no prior information, it is gratifying to observe that it generally agrees well with the

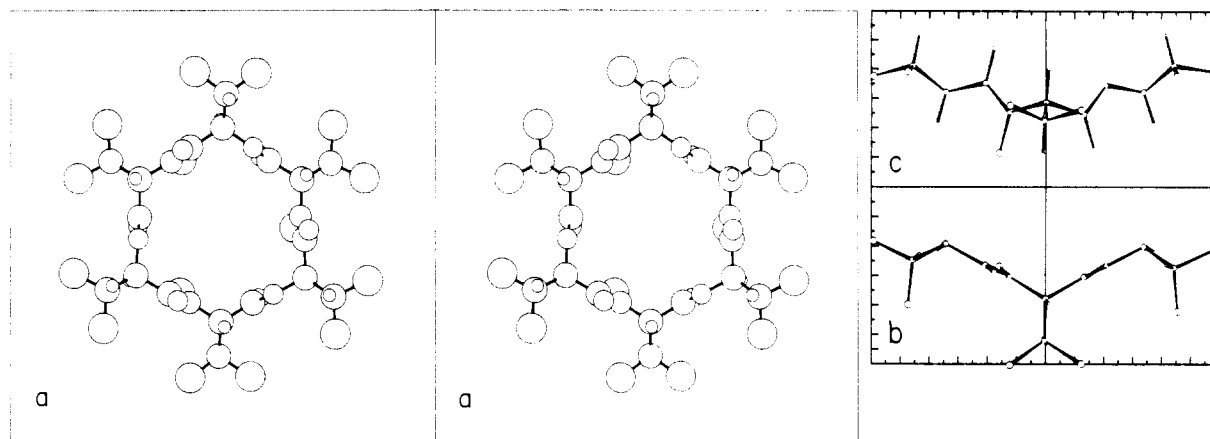


FIGURE 1: Symmetric conformation of EnB, rotamer *t,t*: (a) stereoview; (b) *Y-X* plane projection; (c) *Z-X* plane projection.

experimentally determined conformation in the crystalline state. However, there are also noteworthy differences. The differences between the experimental and calculated  $\phi$  and  $\psi$  values may be attributed to several sources.

First, the force field is approximate, so discrepancies are expected. In particular, the torsional potentials of the angles  $\phi$  and  $\psi$  are known to be rather low. They were set equal to zero in our force field, in view of the lack of a reliable estimate for the intrinsic hindrances to their rotations. Therefore, some coordinated variations in these angles exist, which perhaps violate other constraints only mildly, and therefore cost little energy. However, these constraints involve interactions of the EnB ring with the isopropyl side chains, which reduce considerably the flexibility of the ring, as we shall see below. Second, such coordinated variations may indeed be caused by the crystal packing forces, introducing the observed deviations from perfect  $C_3$  symmetry; therefore, the calculated conformation of a single molecule is *expected* to be different to some extent from that of the molecule in a crystal. Third, the diffraction results are also of limited accuracy, as indicated by an *R* factor of 0.12 and the absence of temperature factors.

Whatever the reasons may be, the calculated  $\phi$  and  $\psi$  values disagree with the experimental ones by up to  $28^\circ$ , but still, they represent quite faithfully the main features of the molecule. The torsion angle  $\omega$  and the out-of-plane angles  $\theta_C$  and  $\theta_N$  pose a more difficult question. By X-ray diffraction, they are exceptionally large, up to  $\sim 24^\circ$ , while in our results (uncomplexed) they are  $3^\circ$  at most. The energy parameters for out-of-plane distortions in our force field were obtained from spectroscopic data and are in reasonable agreement with other experimental data. It seems difficult to suggest a modification of the force field that would produce the reported diffraction results, without conflicting with other experimental data. Either improvements in the X-ray structure determination will reduce the discrepancies, or we are facing an interesting puzzle.

The third row in Table I contains the calculated conformation of the enniatin analogue (LacAla)<sub>3</sub> with methyl side groups replacing the isopropyls of EnB. The differences between the second and third rows, both derived by the same force field, single out the effect of the isopropyl side chains in their lowest energy state on the ring conformation. Differences in  $\phi$ 's and  $\psi$ 's amount up to  $\sim 10^\circ$ , while the out-of-plane angle  $\theta_C$  changed from  $4$  to  $-1^\circ$ . These differences are caused by the interactions of the isopropyls with the amide and ester groups. Indeed, examination of Figure 1 shows that the carbonyls are at contact distances of  $3.2\sim 3.9$  Å from their nearest side-chain methyls and that the *N*-methyl is at a distance of  $3.8$  Å to its nearest side-chain methyl. These

distances are within the repulsive range of the Lennard-Jones potential and reduce significantly the flexibility of EnB according to our force field, and very probably also in reality. (The values of  $r^*$  for O, N, and CH<sub>3</sub> as an "extended atom" in our force field are  $3.65$ ,  $4.01$ , and  $4.17$  Å, respectively).

The fourth row gives the conformation of the same enniatin analogue with the methyl side chains, as calculated by Popov et al. (1970), in the corrected version presented by Ovchinnikov et al. (1974). The differences between our and Ovchinnikov's results are solely due to the differences in the two force fields. First, Popov's calculations involved only 17 variables, while we minimized with respect to all conformational degrees of freedom. Second, there are differences in the details of the energy parameters that comprise the two force fields. We tend to believe that our force field represents a better approximation to reality, reflecting the advances in the empirical force field method in recent years.

**(b) Rotameric States of the Side Chains.** Each isopropyl in EnB has three rotoisomeric (rotameric) states, commonly denoted by *t*, *g*, and *g*<sup>-</sup>, in which the hydrogens of C<sup>α</sup> and C<sup>β</sup> are trans, gauche, and antigauche to each other, respectively. The asymmetric unit of the molecule, having one isopropyl on the hydroxy residue and one on the amino residue, can attain nine states. Table II represents the torsional angles and energy differences of the equilibrium  $C_3$  conformations of enniatin B in seven out of the nine possible symmetric rotamers. The  $C_3$  conformations of the two other rotamers, *g*<sup>-</sup>*g* and *g**g*<sup>-</sup>, are unstable, and their closest equilibrium conformations are unfavorable energetically. It might be deduced from Table II that all the metastable rotamers are so strained as to be insignificant. However, as we shall see below, complex formation may modify the order of stability very significantly. The three rotamers *t,t*, *t,g*, and *g*<sup>-</sup>*t* with lowest energy, as well as rotamers *t,g*<sup>-</sup> and *g*<sup>-</sup>*g*<sup>-</sup>, which have the lowest energy in internal cavity ion complexes, are presented in detail in Figures 1–5. The differences between these rotamers are relatively small, as viewed in the stereoviews, yet they are accompanied by quite large energy differences, which give us some measure of the limited flexibility of the EnB molecule.

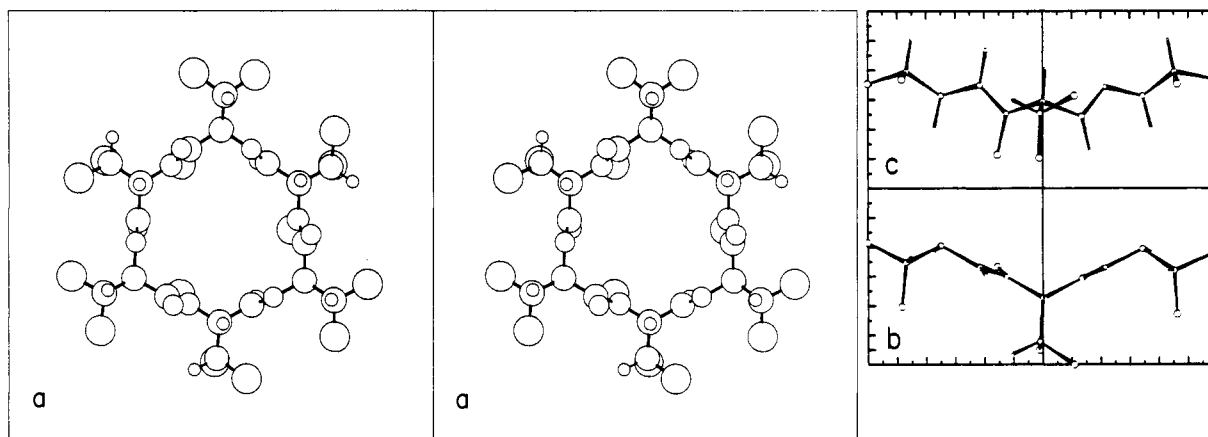
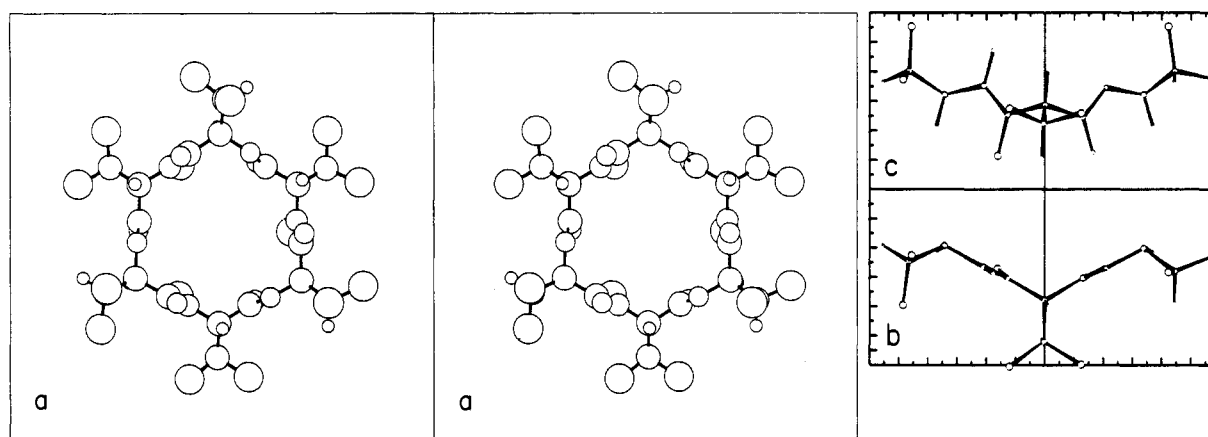
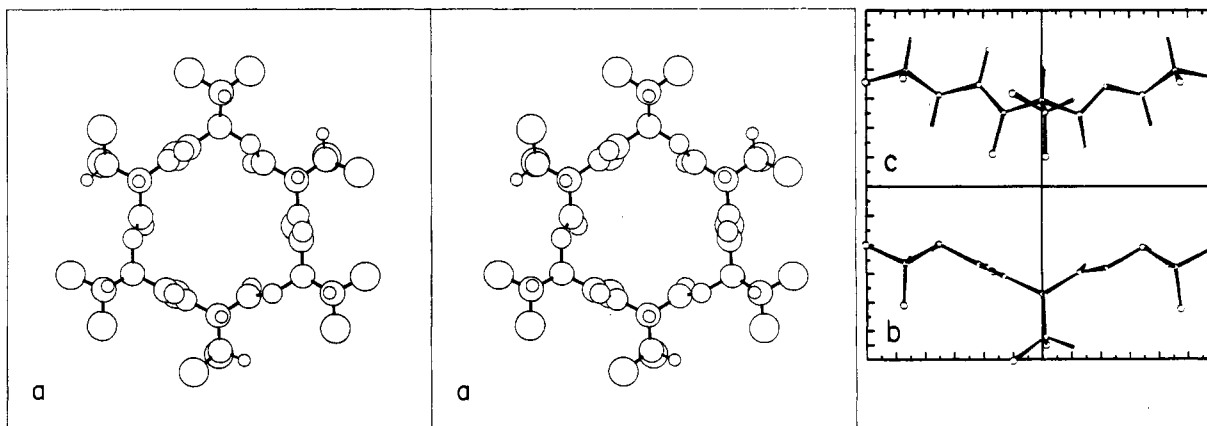
A closer examination of Table II reveals that the HyIV and NMVal residues retain some of their intrinsic character in the various rotamers. Thus, the energies of all nine rotamers can be obtained to a reasonable approximation additively from those of the individual rotamers, if we attribute 8 and 7 kcal/mol to *g* and *g*<sup>-</sup> of the D-HyIV residues and, similarly, 1 and 9 kcal/mol to the corresponding L-NMVal residues, respectively. Furthermore, we find that *g* rotamers tend to bend the carbonyls outward relative to *t*, while in *g*<sup>-</sup>, the carbonyls bend inward. This trend makes the *g*<sup>-</sup> rotamer better

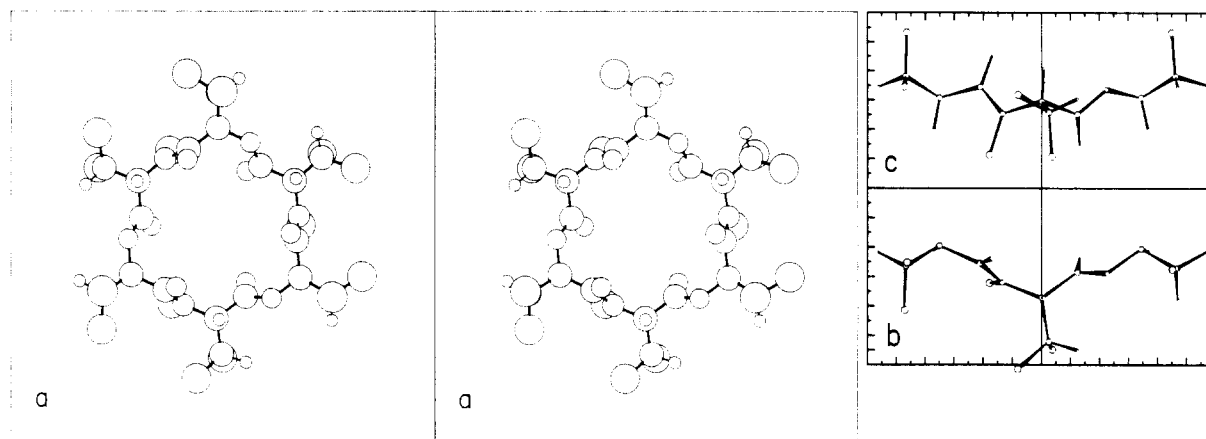
Table II: Symmetric Conformations and Energies of the Isopropyl Rotamers of Enniatin B (deg)

rotamer <sup>a</sup>	$\Delta E$ (kcal/mol)			hydroxyisovaleryl residue				<i>N</i> -methylvalyl residue				
	tot	elec	strain	$\phi$	$\psi$	$\theta_{C'}$	$\omega$	$\theta_N$	$\phi$	$\psi$	$\theta_{C'}$	$\omega$
<i>t,t</i>				112	-98	0	-178	1	-127	112	3	178
<i>t,g</i>	0.8	-3.1	3.8	118	-91	2	179	0	-144	114	-3	-177
<i>g<sup>-</sup>,t</i>	7.1	1.6	5.4	112	-95	0	-178	1	-128	111	4	178
<i>g,g</i>	8.2	-0.4	8.6	122	-81	-4	-179	1	-147	103	-4	180
<i>g,t</i>	8.7	2.7	6.0	117	-89	-4	-176	1	-131	102	0	177
<i>t,g<sup>-</sup></i>	8.9	2.3	6.6	107	-100	2	180	1	-129	121	4	179
<i>g<sup>-</sup>,g<sup>-</sup></i>	15.2	6.9	8.3	71	-132	0	179	10	-87	150	12	180
<i>g<sup>-</sup>,g</i>	6.6	0.4	6.2									
<i>g,g<sup>-</sup></i>	16.9	7.7	9.2									

symmetry is lost by minimization  
symmetry is lost by minimization

<sup>a</sup> The pair of rotamers represents the hydroxy (HyIV) and amino (HMAI) residues, in this order.

FIGURE 2: Symmetric conformation of EnB, rotamer *t,g*: (a-c) as in Figure 1.FIGURE 3: Symmetric conformation of EnB, rotamer *g<sup>-</sup>,t*: (a-c) as in Figure 1.FIGURE 4: Symmetric conformation of EnB, rotamer *t,g<sup>-</sup>*: (a-c) as in Figure 1.

FIGURE 5: Symmetric conformation of EnB, rotamer  $g^-g^-$ : (a-c) as in Figure 1.Table III: Asymmetric Conformations of the Enniatin Ring (deg) and  $\Delta E$  Values<sup>a</sup>

angle	sym	asym 1	asym 2	asym 3	asym 4
Hydroxy Residue					
$\phi$	116	146, 138, 62	96, 65, 128	77, 73, -38	58, 157, 126
$\psi$	-89	55, -81, -130	-105, -144, -83	-116, 53, -63	51, 62, -88
$\theta_{C'}$	0	1, -2, 1	-3, -2, 3	2, 3, -7	0, -1, -1
$\omega$	180	177, 178, 173	-174, 179, -177	172, 176, 180	-175, -177, -177
Amino Residue					
$\theta_N$	0	0, 8, 11	10, 7, 2	11, -2, 3	-5, 4, 9
$\phi$	-137	-45, -105, -92	-83, -97, -149	-65, 68, -141	61, 49, -95
$\psi$	109	66, 117, 107	144, 124, 101	140, -90, 94	83, 57, 129
$\theta_{C'}$	-1	14, 4, 0	10, 3, -1	3, -9, 0	8, 16, 6
$\omega$	-178	177, -176, -176	179, 180, -173	-177, -178, -172	-174, 176, 177
$\Delta E$ (kcal/mol) <sup>b</sup>					
	sym	asym 1	asym 2	asym 3	asym 4
total		-0.9	-0.5	-0.2	0.1
elec		0.3	1.7	-0.1	0.1
strain		-1.2	-2.2	-0.1	0.0
dipole moment	3.95	3.10	4.45	4.85	4.84
dipole moment in CCl <sub>4</sub> <sup>c</sup>		3.35 (3)			

<sup>a</sup> The calculations pertain to the enniatin methyl analogue (LacAla)<sub>3</sub>, with the isopropyl side chains replaced by methyl "extended atoms".<sup>b</sup> Relative to the corresponding energies of the symmetric formation. <sup>c</sup> Ovchinnikov (1974).

suit than  $g$  for ion binding, as may be seen in the next section.

(c) *Asymmetric Conformations and Their Relative Energies.* A number of asymmetric conformations were calculated for the methyl analogue of enniatin. Table III lists the four lowest energy conformations, all within a range of 1 kcal/mol or less, together with the symmetric conformation discussed in the preceding section. Four other metastable conformations of higher energy were also derived. The symmetric conformation was taken as the reference. The electrostatic energy component of the asymmetric conformations in Table III varies within about  $\pm 1$  kcal/mol. This low variability is due to the limited flexibility of the molecule and the restriction of ring closure on the one hand and the long-range nature of Coulomb interactions on the other hand. Thus, if a conformational change pulls two carbonyls apart, it must, in general, bring them nearer to other carbonyls. The conformations listed in Table III do not resemble the five conformations derived by the Russian group [ $N_1$  to  $N_5$  of Table 6 in Ovchinnikov et al. (1974)]. The similarity of energies of the symmetric and the asymmetric conformations may be related to the finding of Grell et al. (1972, 1975) that EnB maintains an equilibrium between different structures in the nonpolar solvent hexane. The values of the dipole moments in these conformations, ranging from 3.1 to 4.8 D, resemble the experimental dipole moment of EnB, 3.35 D in CCl<sub>4</sub> (Ovchinnikov, 1974). One

should bear in mind, however, that these calculations pertain to the enniatin analogue, while the expts. pertain to EnB itself. The behavior in polar solvents is complicated by the solvation of the carbonyl and other groups. Such effects cannot be treated by assuming that the electrostatic intramolecular interaction is inversely proportional to the bulk dielectric constant of the solvent. The theory of electrostatic interactions in solvated systems (Warshel, 1981) may be suitable for this problem.

(II) *Enniatin B-Alkali Ion 1:1 Complexes.* Na<sup>+</sup> and K<sup>+</sup> complexes were calculated for all rotamers of EnB possessing C<sub>3</sub> symmetry. The most stable complexes were selected for performing calculations with the remaining ions, and the results are presented in Table IV. In addition, the alkali ion complexes of the C<sub>3</sub>-symmetric conformers of the methyl analogue (LacAla)<sub>3</sub> and the polylactone analogue Lac<sub>6</sub> (Lifson et al., 1983) are given.

The detailed tables in this section make it possible to draw a great number of comparisons and follow various trends of change in similar systems, by varying one parameter at a time. Because of the complexity of the subject and the many parameters involved, we shall first introduce it by an overview of the main results and conclusions. Consequently, we shall show how these were drawn from the detailed computational data included in Tables IV (1-4) and the accompanying stereo drawings and scaled projections in Figures 6-13. These

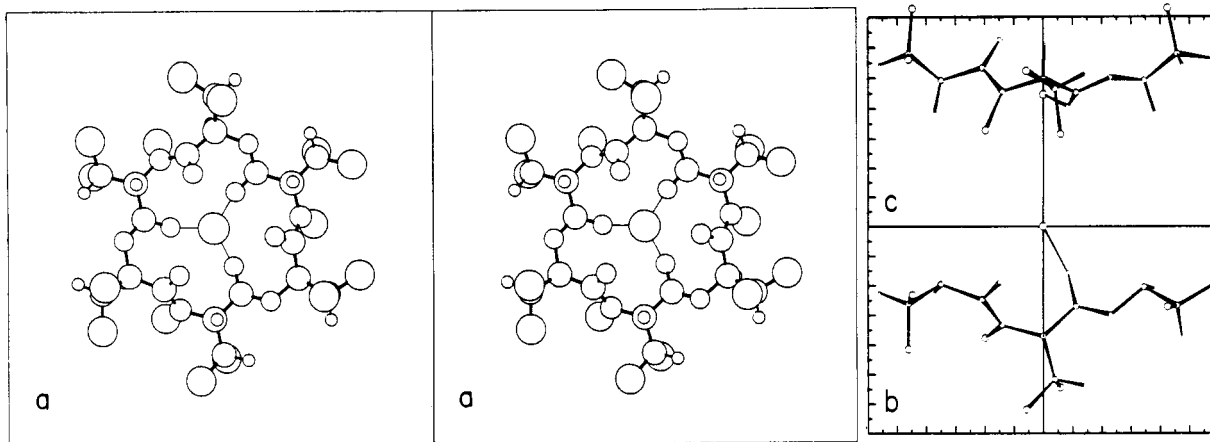


FIGURE 6: EnB-Li<sup>+</sup> 1:1 complex, rotamer  $g^-, g^-$ . Li<sup>+</sup> is bound to NMVal carbonyls.

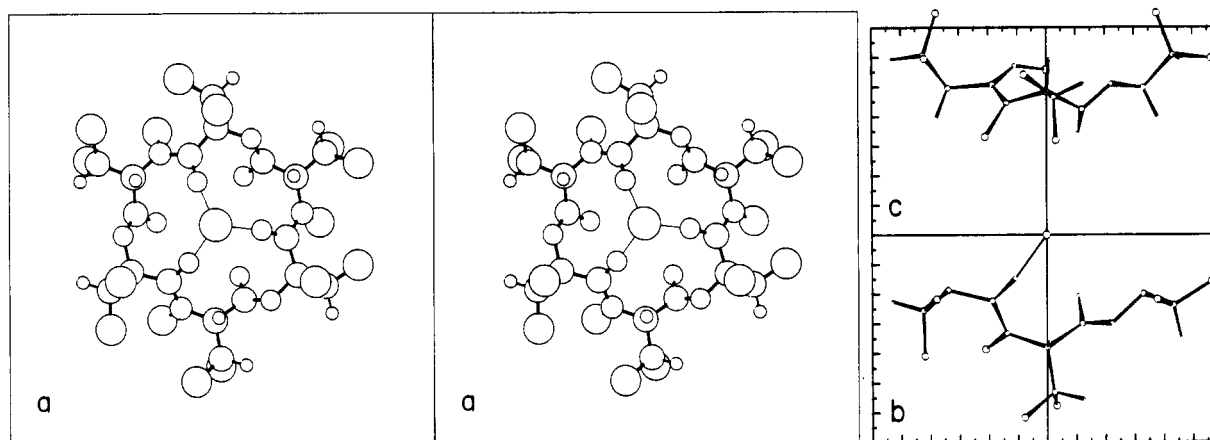


FIGURE 7: EnB-Li<sup>+</sup> 1:1 complex, rotamer  $g^-, g^-$ . Li<sup>+</sup> is bound to HyIV carbonyls.

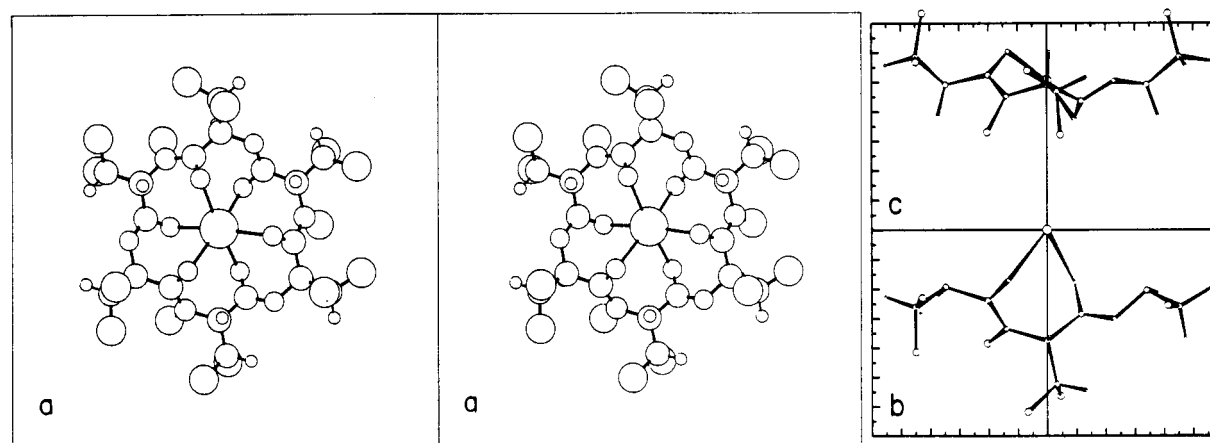


FIGURE 8: EnB-Na<sup>+</sup> 1:1 internal complex, rotamer  $g^-, g^-$ : (a-c) as in Figure 1.

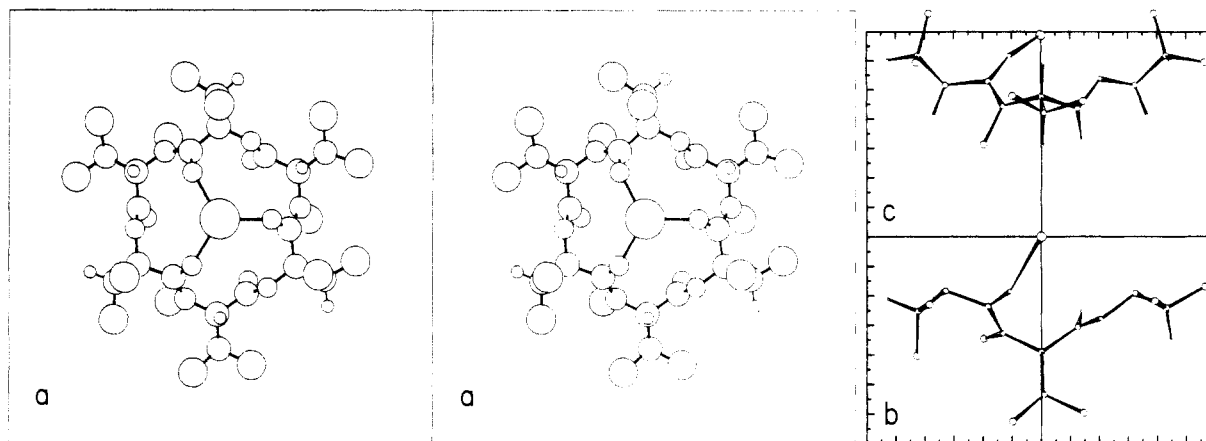
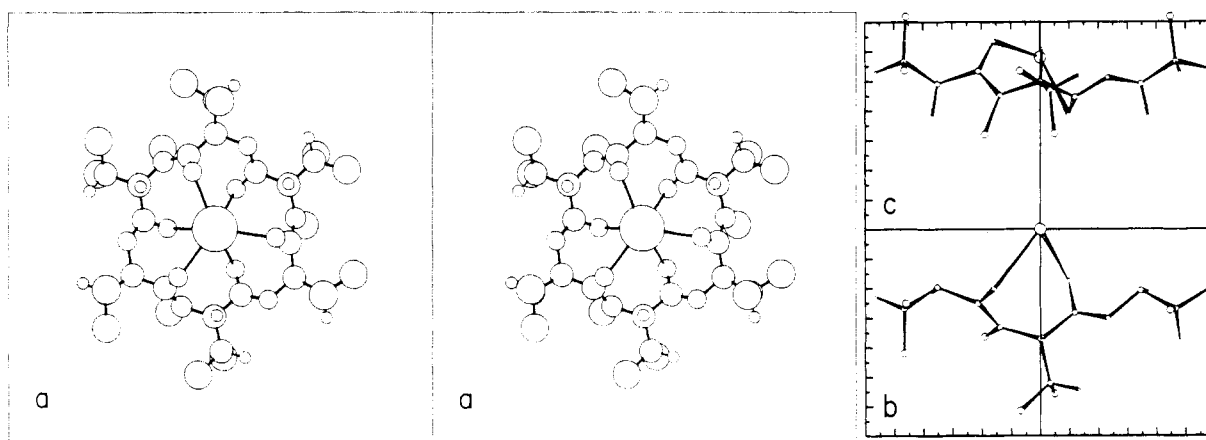
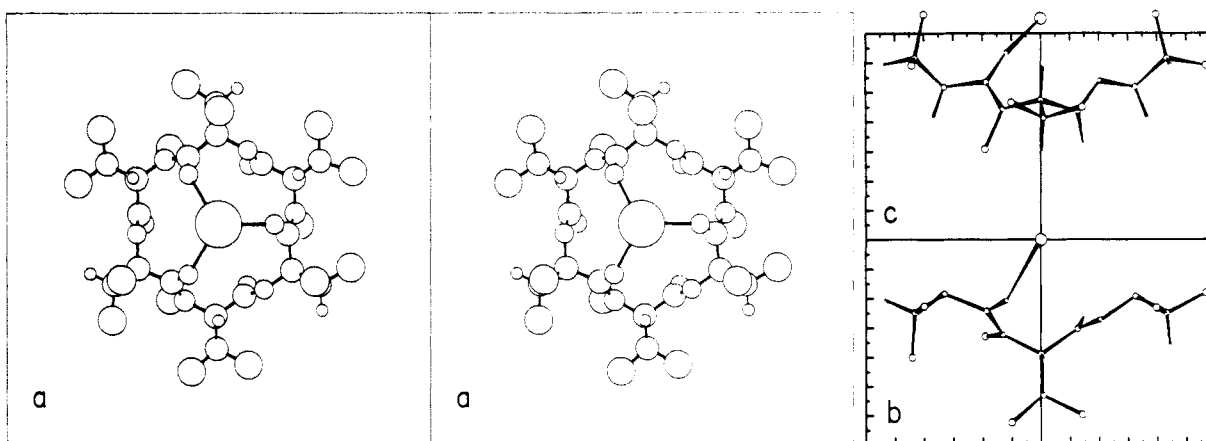
observations are conveniently grouped as follows.

(1) The complexed EnB is found to be highly strained, as compared with the free, unligated molecule. This strain modifies the relative stability of the different rotamers. The complexed EnB is also significantly more strained than the corresponding complexed enniatin analogues studied.

(2) Two distinct kinds of EnB-ion 1:1 complexes, internal and external, are shown to be possible for the medium alkali ions Na<sup>+</sup>, K<sup>+</sup>, and Rb<sup>+</sup>. The smallest alkali ion, Li<sup>+</sup>, binds only internally, while the largest, Cs<sup>+</sup>, binds only externally. In the internal complex, all six carbonyls interact with the ion, while in the external complex only the three carbonyls on one side of the ring, preferentially those of the hydroxyisovaleryl (HyIV) residues, are bound to the ion. Thus, the internal complex possesses a stronger binding (more negative) elec-

trostatic energy. However, this is countbalanced by a higher nonelectrostatic strain energy, since EnB's conformation is highly distorted by inserting a cation in its center, as indicated, inter alia, by large values of the torsion  $\omega$  and out-of-plane  $\theta$  angles. As a consequence of (1) and (2), the energetically preferred rotamers of internal complexes mostly differ from those of external complexes.

(3) The different binding characteristics of particular ions are found to correlate well with the different ionic radii, as expressed in their Lennard-Jones potentials. The Li<sup>+</sup> ion prefers internal binding but is confirmed to be a poor binder altogether. The Na<sup>+</sup> ion fits the cavity better than all other alkali ions and is therefore the best internal binder, but it is also susceptible to external binding. In protic solvents, the externally bound ion remains partially solvated, thus rendering

FIGURE 9: EnB- $\text{Na}^+$  1:1 external complex, rotamer  $g^-, t^-$ : (a-c) as in Figure 1.FIGURE 10: EnB- $\text{K}^+$  1:1 internal complex, rotamer  $g^-, g^-$ : (a-c) as in Figure 1.FIGURE 11: EnB- $\text{K}^+$  1:1 external complex, rotamer  $g^-, t^-$ : (a-c) as in Figure 1.

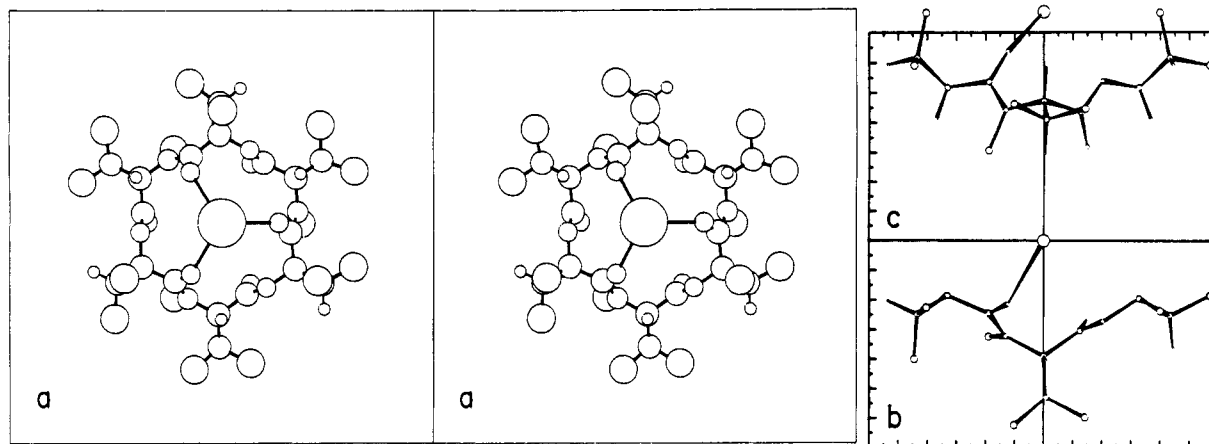
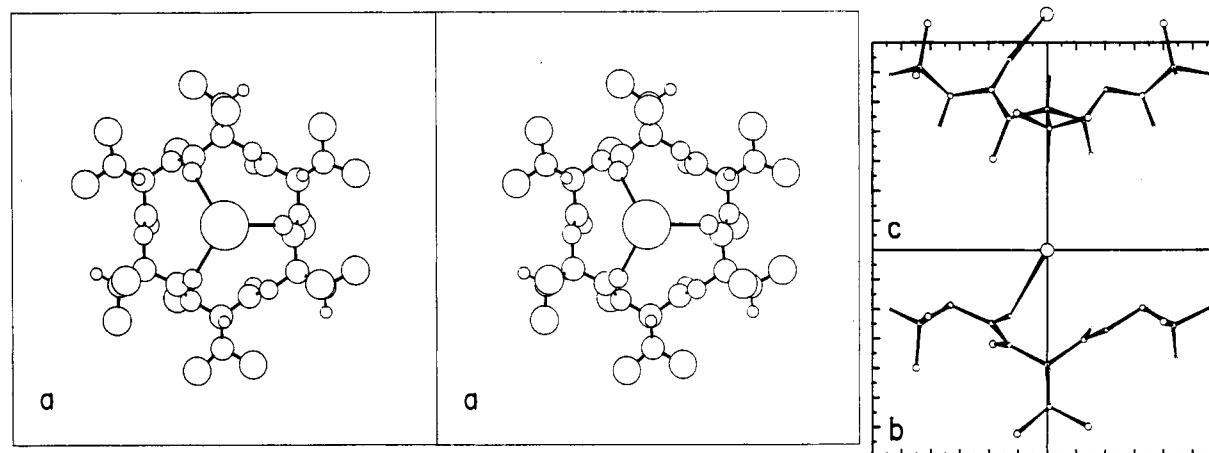
external binding more probable. In purely apolar solvents, the internal binding might be preferred. Among the larger ions,  $\text{K}^+$  and even  $\text{Rb}^+$  can squeeze into the cavity by some "elbow pushing", while  $\text{Cs}^+$  is totally excluded. All the larger ions fit about equally well for external binding, since the variations in binding energy with increasing ionic radius are similar to those in the ionic solvation energy.

As we proceed now to discuss the ion complexes one by one, two guiding remarks might be appropriate. First, the many parameters presented in each table are intimately correlated. It would be tedious and superfluous to discuss everything in detail, and the reader can deduce much information by simply inspecting the tables and figures and comparing them. For example, trends in torsional angles of different rotamers,

different complexes, and different modes of binding and how much they deviate from the torsional angle of the free EnB are better appreciated by scanning the tables than by several pages of discussion.

Second, it should be recognized that items in the tables vary widely as to their level of precision. Important factors in the energy of the complex formation have been omitted, such as solvent effects or the polarization of the ligand by the ion. Thus, for example, the value of the total energy of the complex is useless for direct comparison with experimental enthalpy. However, trends in the variation of the total energies from one complex to another may correspond faithfully to the observable trends. Generally, the trends indicated by comparison of different items within and among tables are more instructive



FIGURE 12: EnB-Rb<sup>+</sup> 1:1 external complex, rotamer *g*<sup>-</sup>,*t*: (a-c) as in Figure 1.FIGURE 13: EnB-Cs<sup>+</sup> 1:1 external complex, rotamer *g*<sup>-</sup>,*t*: (a-c) as in Figure 1.

and more relevant than the items themselves.

(a) *EnB-Li<sup>+</sup> Complex*. Table IV (1), together with figures 6 and 7, presents all pertinent calculated results for the EnB-Li<sup>+</sup> complex. It was observed already in our recent study of polylactone ionophores (Lifson et al., 1983) that the Li<sup>+</sup> ion binds asymmetrically to Lac<sub>6</sub>, the hexalactyl analogue of enniatin, because the cavity is too large and too rigid to let Li<sup>+</sup> contact all carbonyls simultaneously. This is indicated by the distances  $r_0$  between Li<sup>+</sup> and the carbonyl oxygens and by the alignment angles  $\alpha$ :  $r_0$  is shorter and  $\alpha$  is smaller for one side of the ring than for the other side [1.89 Å and 47° vs. 2.48 Å and 70° in the last entry of Table IV (1)]. This trend is even more pronounced in EnB and its methyl analogue (LacAla)<sub>3</sub>. Here the two sides of the ring are distinguishable; the ion makes closer contact either with the amino residues (entries 1 and 2) as, for example, in Figure 6 or with the hydroxy residue (entries 3 and 4) as in Figure 7. This kind of poor fitting of the Li<sup>+</sup> in the cavity puts the solvation of the Li<sup>+</sup> by the ionophore at a disadvantage relative to its solvation by the solvent.

(b) *EnB-Na<sup>+</sup> Complex*. Table IV (2) and figures 8 and 9 summarize the results for the Na<sup>+</sup> complexes. Here, the most striking observation is the existence of two modes of binding, internal and external. In so far as the solvent is ignored, the internal mode is by ~6 kcal/mol more stable, within the accuracy of our force field. They differ also in other respects. The electrostatic energy is much larger (more negative) for the internal complex, since the Na<sup>+</sup> ion binds equally well to all six carbonyls, while the external binding involves only three carbonyls, preferably those of the D-HyIV residues. However, the Na<sup>+</sup>-oxygen distance  $r_0$  of the external

binding is shorter by ~0.1 Å and the alignment angle smaller by ~30°, thus making the specific binding per carbonyl stronger. Furthermore, the internal complex is more strained than the external one: its nonelectrostatic energy is larger by ~12 kcal/mol, and its molecular conformation is more distorted, compared to that of free EnB or to the external complex.

The internal binding parameters for Na<sup>+</sup> show that this ion fits the EnB cavity better than any other alkali ion. It sits right at the center of the cavity (Figure 8). Its Na<sup>+</sup>-oxygen distances  $r_0$  and  $\alpha$  angles are almost equal for the amino and the hydroxy carbonyls. Remembering that solvent effects are not included and that our force field ignores the polarization energy, which, like the Coulomb interaction, might be larger for the internal binding, one should expect the internal complex of EnB-Na<sup>+</sup> to be more stable in apolar or aprotic solvents. On the other hand, in polar solvents, and protic solvents like alcohols in particular, since the external binding leaves one side of the ion exposed to the solvent, partial solvation is expected to be sufficiently large to tip the balance over in favor of external binding. Note that the methyl side chain analogue of EnB is more stable by ~6 kcal/mol than EnB itself for internal binding and does not show a stable external complex according to our calculation. This indicates the important contribution of the isopropyl side chains to the nonelectrostatic strain energy, which is so much larger in the case of the internal complex than that of the external one. Note also that the rotamers that yield the best internal binding are different from those that are preferred for external binding.

(c) *EnB-K<sup>+</sup> Complex*. The results for this complex are summarized in Table IV (3) and in Figures 10 and 11. Po-

Table IV: Alkali Ion 1:1 Complexes with Enniatin B and Methyl Analogues: Energies, Geometric Parameters, and Conformations

ligand (rotamer) <sup>a</sup>	$\Delta E$ (kcal/mol) <sup>b</sup>				geometric parameters (Å)					conformation (deg)					
	tot	elec	strain		$r_o^c$	$2x^{1/2}$	$r_2^d$	$r_1^e$	$\alpha^f$	$\chi$	$\theta_N$	$\phi$	$\psi$	$\theta_{C'}$	$\omega$
(1) Lithium Ion 1:1 Complex															
EnB ( <i>t</i> , <i>g</i> <sup>-</sup> ) <sup>g</sup>	-67	-93	26	HyIV	2.96	4.18	3.88	3.05	85	-171		41	-126	9	180
				NMVal	1.81	2.56	3.09	2.98	40	-57	-3	-65	155	-8	-179
EnB ( <i>g</i> <sup>-</sup> , <i>g</i> <sup>-</sup> ) <sup>g</sup>	-67	-95	28	HyIV	2.71	3.83	3.75	2.94	77	-62		42	-132	11	179
				NMVal	1.86	2.63	3.10	2.89	44	-57	-3	-63	157	-10	-177
EnB ( <i>g</i> <sup>-</sup> , <i>g</i> <sup>-</sup> ) <sup>h</sup>	-66	-93	27	HyIV	1.85	2.61	3.14	3.00	41	-64		54	-146	3	-170
				NMVal	2.88	4.08	3.83	2.98	83	-60	-2	-58	137	-17	-173
(LacAla) <sub>3</sub> <sup>h</sup>	-81	-99	18	Lac	1.82	2.58	3.05	2.89	39			58	-155	5	179
				NMAla	2.76	3.90	3.86	2.94	82		-8	-38	127	-11	-178
Lac <sub>6</sub>	-75	-95	20	D-Lac	2.48	3.51	3.41	2.86	70			50	-135	22	-173
				L-Lac	1.89	2.67	3.06	2.88	47			-58	147	-17	170
(2) Sodium Ion 1:1 Complex															
Internal Cavity Binding															
EnB ( <i>t</i> , <i>g</i> )	-57	-80	23	HyIV	2.35	3.32	3.51	3.07	67	-170		56	-136	7	-176
				NMVal	2.33	3.30	3.56	3.05	67	69	-5	-59	136	-16	180
EnB ( <i>g</i> <sup>-</sup> , <i>g</i> <sup>-</sup> )	-52	-79	27	HyIV	2.34	3.31	3.64	3.10	64	-64		55	-141	10	-178
				NMVal	2.36	3.33	3.52	2.99	65	-55	0	-72	154	-19	-172
EnB ( <i>t</i> , <i>g</i> <sup>-</sup> )	-51	-76	25	HyIV	2.37	3.35	3.67	3.13	66	-170		56	-139	8	-177
				NMVal	2.35	3.32	3.49	3.01	65	-55	-1	-72	151	-20	174
(LacAla) <sub>3</sub>	-63	-80	17	Lac	2.32	3.28	3.41	2.99	62			61	-152	10	178
				NMAla	2.34	3.31	3.70	3.01	65		-8	-56	144	-12	-177
Lac <sub>6</sub>	-57	-79	22	D-Lac	2.30	3.25	3.45	3.05	63			65	-144	21	-172
				L-Lac	2.30	3.25	3.45	4.05	63			-65	144	-21	172
External Binding to the D-Hydroxyvaleryl Carbonyls															
EnB ( <i>g</i> <sup>-</sup> , <i>t</i> )	-51	-62	11	HyIV	2.25	3.19	3.66		32	-62		79	-140	1	-172
				NMVal						175	4	-70	124	-4	178
EnB ( <i>t</i> , <i>t</i> )	-50	-58	8	HyIV	2.27	3.21	3.76		37	-172		84	-137	1	-171
				NMVal						176	4	-74	120	-6	177
EnB ( <i>g</i> , <i>t</i> )	-48	-59	11	HyIV	2.24	3.17	3.60		28	63		88	-152	-2	-174
				NMVal						175	5	-68	124	-6	178
(LacAla) <sub>3</sub>	-56	-63	7	Lac	2.22	3.17	3.65		28			75	-152	-1	-179
				NMAla							3	-61	135	-9	179
Lac <sub>6</sub>	-50	-60	10	D-Lac	2.23	3.16	3.30		27			67	-145	0	177
				L-Lac								-57	132	-15	-177
(3) Potassium Ion 1:1 Complex															
Internal Cavity Binding															
EnB ( <i>t</i> , <i>g</i> )	-38	-58	20	HyIV	2.62	3.70	4.32	3.37	72	-172		70	-130	9	179
				NMVal	2.74	3.87	3.61	3.55	77	76	3	-83	146	-22	180
EnB ( <i>t</i> , <i>g</i> <sup>-</sup> )	-32	-54	22	HyIV	2.62	3.70	4.41	3.54	69	-172		65	-131	9	178
				NMVal	2.74	3.88	3.46	3.27	75	-52	3	-88	157	-23	-176
(LacAla) <sub>3</sub>	-42	-57	15	Lac	2.58	3.65	4.40	3.44	65			66	-136	9	173
				NMAla	2.77	3.92	3.40	3.24	74		5	-83	159	-22	-176
Lac <sub>6</sub>	-35	-56	21	D-Lac	2.84	4.02	3.05	3.17	71			63	-132	14	169
				L-Lac	2.57	3.64	4.46	3.31	59			-78	156	-22	-179
External Binding to the D-Hydroxyvaleryl Carbonyls															
EnB ( <i>t</i> , <i>t</i> )	-40	-43	3	HyIV	2.66	3.76	4.18		39	-173		90	-129	2	-174
				NMVal						177	5	-83	117	-3	175
EnB ( <i>g</i> <sup>-</sup> , <i>t</i> )	-40	-47	7	HyIV	2.64	3.73	3.99		32	-60		83	-134	1	-174
				NMVal						177	6	-76	123	0	176
EnB ( <i>t</i> , <i>g</i> )	-38	-46	8	HyIV	2.63	3.72	4.12		35	-171		79	-135	-1	-176
				NMVal						72	7	-76	129	-8	176
EnB ( <i>g</i> , <i>t</i> )	-36	-43	7	HyIV	2.63	3.72	3.89		27	64		90	-145	-2	-175
				NMVal						177	7	-73	123	-2	176
(LacAla) <sub>3</sub>	-43	-45	2	Lac	2.63	3.71	3.93		27			78	-142	-2	-178
				NMAla							6	-70	131	-4	178
Lac <sub>6</sub>	-38	-44	6	D-Lac	2.63	3.72	3.71		23			68	-143	4	178
				L-Lac								-58	132	11	-179
(4) Rubidium and Cesium Ion 1:1 Complexes															
Internal Cavity Binding: Rubidium															
EnB ( <i>t</i> , <i>g</i> )	-33	-51	18	HyIV	2.71	3.89	4.64	3.43	70	-172		71	-127	8	176
				NMVal	2.95	4.17	3.51	3.65	81	77	5	-87	149	-22	178
EnB ( <i>g</i> <sup>-</sup> , <i>g</i> <sup>-</sup> )	-27	-50	23	HyIV	2.69	3.80	4.65	3.54	63	-61		64	-131	9	174
				NMVal	2.96	4.19	3.32	3.26	77	-51	6	-88	164	-21	-177
(LacAla) <sub>3</sub>	-39	-55	16	Lac	2.71	3.83	4.68	3.28	70			70	-162	9	-174
				NMAla	2.94	4.15	3.11	3.16	62		-13	-51	130	-1	-177
External Binding to the D-Hydroxyvaleryl Carbonyls															
(a) Complexes with Rubidium Ion															
EnB ( <i>t</i> , <i>t</i> )	-37	-39	2	HyIV	2.78	3.93	4.31		40	-174		92	-126	2	-174
				NMVal						178	5	-85	117	-2	175

Table IV (Continued)

ligand (rotamer) <sup>a</sup>	$\Delta E$ (kcal/mol) <sup>b</sup>				geometric parameters (Å)					conformation (deg)					
	tot	elec	strain		$r_o^c$	$2x^{1/2}$	$r_2^d$	$r_1^e$	$\alpha^f$	$\chi$	$\theta_N$	$\phi$	$\psi$	$\theta_{C'}$	$\omega$
EnB ( $g^-,t$ )	-37	-43	6	HyIV	2.76	3.90	4.08		32	-60		84	-132	1	-175
				NMVal						177	6	-77	123	1	176
(LacAla) <sub>3</sub>	-40	-41	1	Lac	2.76	3.90	4.04		28			79	-138	-1	-177
				NMAla							7	-73	130	-3	178
(b) Complexes with Cesium Ion															
EnB ( $t,t$ )	-34	-35	1	HyIV	2.98	4.21	4.48		40	-174		94	-123	2	-175
				NMVal						178	5	-89	116	-1	175
EnB ( $g^-,t$ )	-34	-38	4	HyIV	2.95	4.18	4.20		31	-59		85	-130	1	-175
				NMVal						177	6	-80	122	2	175
(LacAla) <sub>3</sub>	-37	-36	-1	Lac	2.96	4.18	4.20		29			80	-133	-1	-177
				NMAla							8	-77	128	-2	178

<sup>a</sup> See text for abbreviations contained herein. <sup>b</sup> Relative to the reference energies of the rotamer  $t,t$  of the uncomplexed ligand. See Table II. Elec and strain are the electrostatic and strain energies, respectively. <sup>c</sup> Ion to carbonyl oxygen distance. <sup>d</sup> Distance between next nearest neighbor carbonyl oxygens. <sup>e</sup> Distance between nearest-neighbor carbonyl oxygens. <sup>f</sup> Angle between bond vectors (ion-O') and (O'=C'). <sup>g</sup> Li<sup>+</sup> binds to the amino acyl residue. For rotamer  $t,g$ , this is the only stable binding conformation. <sup>h</sup> Li<sup>+</sup> binds to the hydroxy acyl residue. For the analogue (LacAla)<sub>3</sub>, this is the only stable binding conformation.

tassium, like sodium, can bind to EnB both internally (Figure 10) and externally (Figure 11). Here, however, the calculated energy of the most stable external complex is stronger by 8 kcal/mol than that of the corresponding internal complex. The internal binding complex is characterized by a distorted cavity, originating from the K<sup>+</sup> ion being too large to be accommodated comfortably and symmetrically in the cavity. Unlike the Li<sup>+</sup> case, all carbonyls make close contacts with K<sup>+</sup>, but the pyramid formed by the K<sup>+</sup> as apex and the three hydroxy residue carbonyls as base is distinct from the corresponding pyramid with the amino residue carbonyls. The  $r_2$  distance between the NMVal carbonyls is smaller by  $\sim 1$  Å than the  $r_2$  between the HyIV carbonyls, as the K<sup>+</sup> ion is squeezed asymmetrically closer to the HyIV carbonyls. The asymmetric squeezing is about as pronounced in the enniatin analogues, and was noted already (Lifson et al., 1983) for Lac<sub>6</sub>.

The external EnB complex of K<sup>+</sup> does not differ much from that of Na<sup>+</sup>. It has a smaller non-Coulombic strain energy and comparable alignment angles. When comparing conformations of the external complexes of K<sup>+</sup> and Na<sup>+</sup> with the most stable conformation of the free EnB, the  $t,t$  rotamer, one observes that the K<sup>+</sup> complex is less distorted than the Na<sup>+</sup> one.

The foregoing considerations, supported by further detailed comparison of Table IV (2 and 3), indicate consistently that internal binding is less favorable in the K<sup>+</sup> case than in the Na<sup>+</sup> case. Since it is also less favorable than the external binding of the same K<sup>+</sup> ion, it is to be expected that K<sup>+</sup> may bind externally in all solvents, which is in accord with the observation (Ivanov, 1973; Ovchinnikov et al., 1974) that K<sup>+</sup>, and not Na<sup>+</sup>, tends to form 2:1 sandwich complexes in concentrated alcohol solution or in transport through lipid bilayers at all concentrations. We shall return to this point in the next section on dimer complexes.

(d) *Rb<sup>+</sup> and Cs<sup>+</sup> Complexes.* The results are given in Table IV (4) and Figures 12 and 13. Although our force field accommodated even Rb<sup>+</sup> internally, the external binding of Rb<sup>+</sup> seems so much more favorable than internal binding might be altogether unobservable. Internal binding of Cs<sup>+</sup> is found to be unstable. External binding of these ions is quite similar to that of K<sup>+</sup>. The binding energy decreases slowly with increasing ionic radius, in a manner similar to the ionic solvation energies. These considerations are borne out by the fact that the measured binding constants of K<sup>+</sup>, Rb<sup>+</sup>, and Cs<sup>+</sup> are quite similar, indicating very small differences in the free energies of binding.

(III) *Dimer-Ion (2:1) Complexes.* It was noted already that when an ion forms an external complex with EnB, it is in part exposed to the solvent. The solvent may however be replaced by a second EnB molecule, such that six carbonyls, three from each EnB molecule, engulf the ion into an octahedral cage. Indeed, Ivanov et al. (1973) observed such dimer complexes. We examined EnB dimer complexes, consisting of either the  $t,t$  or  $g^-,t$  rotamers, since the external 1:1 complexes of these rotamers are the most stable. The conformations of the dimer complex were constrained throughout the calculations to retain C<sub>3</sub> rotation symmetry, with the ion lying along the rotation axis symmetrically located between the ligands. This device saved computer time without biasing the results, since both symmetric conformations are found to be stabilized by many interatomic contacts between the two ligand molecules.

The conformations of EnB in the dimer complexes are given in Table V. They are similar to those of the corresponding rotamers in the external 1:1 complexes yet sufficiently different to exhibit the effect of the dimer interactions. Figures 14 and 15 give the stereoviews of the K<sup>+</sup> complexes for the rotamers  $t,t$  and  $g^-,t$ , viewed along the Z and Y axes. The stereoviews of the other 2:1 complexes are quite similar.

The energies of the dimer complexes and the geometric parameters of the dipolar cavities engulfing the complexed ions are given in Table VI. The total energy of the dimer complex and its electrostatic and nonelectrostatic components are separated into two parts.  $\Delta E_1$  represents the formation of the 1:1 complex from a free ligand and an ion, as presented in Table IV (2-4).  $\Delta E_2$  represents the formation of the dimer from the 1:1 complex and the second free ligand. As already pointed out, the calculated energies are, by themselves, not sufficiently accurate to be meaningful, since solvation and polarization effects have been ignored; however, their relative changes are instructive. All the ions in Table VI exhibit common trends.  $\Delta E_1$ (total) values are the same for the rotamers  $t,t$  and  $g^-,t$  while  $\Delta E_2$  values of  $t,t$  are larger (more negative), probably due to better contact between the side chains.  $\Delta E_2$  is more negative than  $\Delta E_1$  for K<sup>+</sup>, Rb<sup>+</sup>, and Cs<sup>+</sup>. This suggests a preference of dimer over monomer binding, in so far as only the energetic factors included in our calculations are concerned. For Na<sup>+</sup>, on the other hand, since  $\Delta E_2$ (total) is less negative than  $\Delta E_1$ , dimer binding is less favored. These conclusions are qualitative agreement with experiment (Ovchinnikov et al., 1974).

Various other differences between 1:1 and 2:1 binding are observed by examining the geometric parameters of the com-

Table V: Alkali Ion 2:1 Complexes of Enniatin B: Conformations (deg)<sup>a</sup>

		hydroxyisovaleryl residue					N-methylvaleryl residue					
ion	rotamer	$\chi$	$\phi$	$\psi$	$\theta_{C'}$	$\omega$	$\chi$	$\theta_N$	$\phi$	$\psi$	$\theta_{C'}$	$\omega$
Na <sup>+</sup>	<i>t,t</i>	180	86	-148	-5	-168	176	7	-72	122	-1	179
	<i>g<sup>-</sup>,t</i>	-62	88	-149	2	-175	178	8	-77	131	1	-179
K <sup>+</sup>	<i>t,t</i>	-170	76	-133	-4	-169	176	6	-71	119	3	177
	<i>g<sup>-</sup>,t</i>	-62	86	-144	1	-175	177	7	-78	130	2	180
Rb <sup>+</sup>	<i>t,t</i>	-171	79	-130	-3	-171	176	6	-75	119	3	176
	<i>g<sup>-</sup>,t</i>	-61	84	-141	1	-175	178	6	-85	116	2	174
Cs <sup>+</sup>	<i>t,t</i>	-176	92	-123	0	-175	178	6	-85	116	3	174
	<i>g<sup>-</sup>,t</i>	-60	82	-135	0	-175	177	7	-78	127	5	177

<sup>a</sup> Both ligands of the complex have identical conformations.

Table VI: Alkali Ion 2:1 Complexes of Enniatin B: Energies and Geometric Parameters

ion	rotamer		$\Delta E$ (kcal/mol) <sup>a</sup>			geometric parameters (Å) <sup>b</sup>			
			tot	elec	strain	$r_0^c$	$r_2^d$	$r_3^e$	$\alpha^f$
Na <sup>+</sup>	<i>t, t</i>	$\Delta E_1$	-50	-58	8	2.27	3.21		37
		$\Delta E_2$	-48	-20	-28	2.51	3.55	2.90, 4.31	23
	<i>g<sup>-</sup>, t</i>	$\Delta E_1$	-51	-62	11	2.25	3.19		32
		$\Delta E_2$	-38	-14	-24	2.66	3.76	3.15, 4.63	19
K <sup>+</sup>	<i>t, t</i>	$\Delta E_1$	-40	-43	3	2.66	3.76		49
		$\Delta E_2$	-51	-31	-20	2.67	3.77	3.03, 4.70	30
	<i>g<sup>-</sup>, t</i>	$\Delta E_1$	-40	-47	7	2.64	3.73		32
		$\Delta E_2$	-43	-24	-19	2.78	3.94	3.34, 4.88	21
Rb <sup>+</sup>	<i>t, t</i>	$\Delta E_1$	-37	-39	2	2.78	3.93		40
		$\Delta E_2$	-48	-30	-18	2.75	2.89	3.07, 4.79	32
	<i>g<sup>-</sup>, t</i>	$\Delta E_1$	-37	-43	6	2.76	3.90		32
		$\Delta E_2$	-43	-26	-17	2.85	4.03	3.45, 5.01	23
Cs <sup>+</sup>	<i>t, t</i>	$\Delta E_1$	-34	-35	1	2.98	4.21		40
		$\Delta E_2$	-44	-26	-18	2.98	4.21	3.20, 4.86	40
	<i>g<sup>-</sup>, t</i>	$\Delta E_1$	-34	-38	4	2.95	4.18		31
		$\Delta E_2$	-40	-26	-14	2.97	4.20	3.67, 5.31	26

<sup>a</sup> The total, electrostatic, strain energies have the *t,t* rotamer of the uncomplexed ligand as the reference state, as in Table II.  $\Delta E_1$  is the incremental energies associated with binding a single ligand to the ion [taken from Table IV (2-4)];  $\Delta E_2$  is the incremental energies associated with binding a second ligand of the same conformation to the 1:1 complex. <sup>b</sup> Alternate lines give the values for the 1:1 complex from Table IV (2-4) and the values for the corresponding 2:1 complex. <sup>c</sup> Ion to carbonyl oxygen distance (HyIV). <sup>d</sup> Distance between binding carbonyl oxygens residing on the same ring. <sup>e</sup> Distances between adjacent binding carbonyl oxygens residing on different rings. <sup>f</sup> Angle between bond vectors (ion-O') and (O'=C').

Table VII: Alkali Ion 2:1 Complexes of Enniatin B: Inter-Methyl Contact Distances (Å) between the Rings<sup>a</sup>

ion	rotamer <i>g<sup>-</sup>,t</i>			rotamer <i>t,t</i>	
	HyIV(ax)- HyIV(ax) <sup>b</sup>	HyIV(ax)- HyIV(eq) <sup>c</sup>	HyIV(ax)- NMVal(eq) <sup>c</sup>	HyIV(eq)- HyIV(eq) <sup>b</sup>	HyIV(eq)- NMVal(eq) <sup>c</sup>
Na <sup>+</sup>	3.35	3.87	3.59	3.32	4.03
K <sup>+</sup>	3.51	4.07	3.84	3.65	
Rb <sup>+</sup>	3.62	4.19	4.00	3.65	
Cs <sup>+</sup>	4.03			3.52	

<sup>a</sup> The notation used is (ax) a methyl group positioned axially with respect to the ring plane (e.g., trans with respect to H of C<sup>α</sup>) and (eq) a methyl group positioned equatorially with respect to the ring plane. <sup>b</sup> There are three such contact distances per complex. <sup>c</sup> There are six such contact distances per complex.

plexes. The carbonyl-ion distances are always somewhat larger in the dimer complex, while the alignment of the carbonyls toward the ion is better. The cavity formed by the dimer differs significantly from that formed by internal 1:1 binding. In the Na<sup>+</sup> internal complex, the distances of a carbonyl to its two first neighbors [ $r_1$  in Table IV (2)] are almost the same, and consequently, the carbonyls on one side of the ring are almost perfectly staggered with respect to those on the other side, as viewed along the symmetry axis (Figure 8). In the dimer complex, the corresponding carbonyl-carbonyl distances  $r_3$  are different, and the carbonyls of one ligand are halfway between staggered and eclipsed with respect to the other ligand (Figures 14 and 15).

It seems that this relative positioning of two ligands is determined mainly by the contacts made between their side chains, which are tabulated in Table VII. Although these

contacts are mostly in the repulsive range, the contribution of strain energy to the dimer formation,  $\Delta E_2$ (strain), is negative and large as compared to that of the 1:1 complex,  $\Delta E_1$ (strain). Moreover, it appears that most of these contacts involve the isopropyl side chains of the HyIV residues, which are conserved among the family of naturally occurring enniatins.

#### Added in Proof

We are grateful to Dr. Dobler for kindly calling our attention to recent crystallographic determinations of free, unhydrated EnB (Dobler, 1981) and of hydrated EnB (EnB·1<sup>1</sup>/<sub>2</sub>H<sub>2</sub>O; Tishchenko et al., 1982) that regrettably escaped us. It is gratifying to note that the large out-of-plane torsions in Tishchenko et al. (1976) quoted in Table I have been proven artifacts, as predicted by us. Dr. Dobler also noted that our

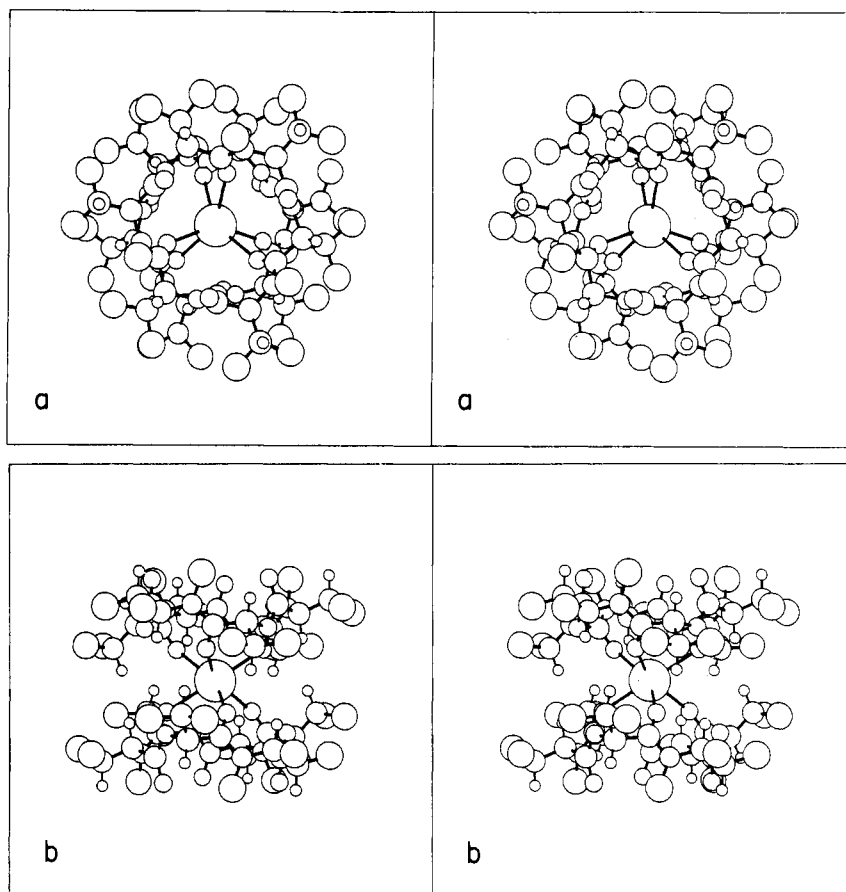


FIGURE 14: EnB-K<sup>+</sup> 2:1 complex, rotamer *t,t*. Stereoviews (a) along the symmetry (*Z*) axis and (b) along the *Y* axis.

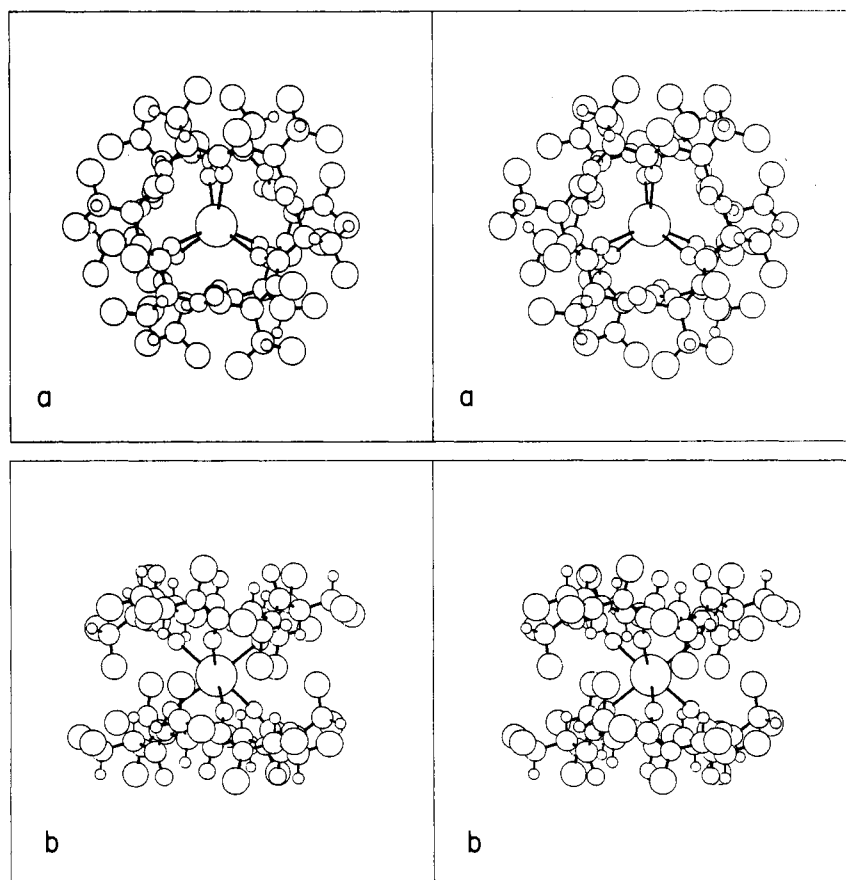


FIGURE 15: EnB-K<sup>+</sup> 2:1 complex, rotamer *g<sup>-</sup>,t*. Stereoviews (a and b) as in Figure 14.

calculated conformation of free unhydrated EnB resembles the experimental conformation of hydrated EnB better than that of the unhydrated one. A possible solution of this puzzle will be discussed elsewhere. We are also grateful to Dr. Benz for kindly calling our attention to EnB-mediated ion transport experiments (Benz, 1978), showing 1:1 complexing ratios where Ivanov et al. (1973) found 2:1 ratios. Our calculations indicate the possibility of both 2:1 and 1:1 ratios but are short of predicting the precise corresponding binding constants.

**Registry No.** EnB, 917-13-5; (LacAla)<sub>3</sub>, 56760-72-6.

## References

- Benz, R. (1978) *J. Membr. Biol.* **43**, 367.  
 Buckingham, R. A. (1937) *Proc. R. Soc. London, Ser. A* **160**, 113.  
 Burgermeister, W., & Winkler-Oswatitsch, R. (1977) in *Topics in Current Chemistry, Inorganic Biochemistry II*, Vol. 69, p 91, Springer-Verlag, Berlin.  
 Dobler, M. (1981) *Ionophores and Their Structures*, Wiley, New York.  
 Dobler, M., Dunitz, J. D., & Krajewski, J. (1969) *J. Mol. Biol.* **42**, 603.  
 Felder, C. E., Shanzer, A., & Lifson, L. (1984) *J. Comput. Chem.* (in press).  
 Grell, E., Eggers, F., & Funck, T. (1972) *Chimia* **26**, 632.  
 Grell, E., Funck, T., & Eggers, F. (1975) *Membranes, A Series of Advances* (Eisenman, G., Ed.) p 47, Marcel Dekker, New York.  
 Gurevich, A. Z. (1980) *Bioorg. Khim.* **6**, 197.  
 Hagler, A. T., Stern, P. S., Sharon, R., Becker, J. M., & Naider, F. (1979) *J. Am. Chem. Soc.* **101**, 6842.  
 Ivanov, V. T., Evstratov, A. V., Sumskaya, L. V., Melnik, E. I., Chumburidze, T. S., Portnova, S. L., Balashova, T. A., & Ovchinnikov, Y. A. (1973) *FEBS Lett.* **36**, 65.  
 Ketelaar, J. A. A. (1953) *Chemical Constitution*, p 28, Elsevier, Amsterdam.  
 Lifson, S. (1983) in *Supramolecular Structure and Function* (Pifat, G., & Herak, J. N., Eds.) p 1, Plenum Press, New York.  
 Lifson, S., Hagler, A. T., & Dauber, P. (1979) *J. Am. Chem. Soc.* **101**, 5111.  
 Lifson, S., Felder, C. E., & Shanzer, A. (1983) *J. Am. Chem. Soc.* **105**, 3866.  
 Motherwell, S. (1979) *Computer Code PLUTO*, University Chemical Laboratory, Cambridge, England.  
 Noyes, R. M. (1962) *J. Am. Chem. Soc.* **84**, 513.  
 Ovchinnikov, Y. A. (1974) *FEBS Lett.* **44**, 1.  
 Ovchinnikov, Y. A., & Ivanov, V. T. (1982) *Proteins (3rd Ed.)* **5**, 365.  
 Ovchinnikov, Y. A., Ivanov, V. T., Evstratov, A. V., Mikhaileva, I. I., Bystrov, V. F., Portnova, S. L., Balashova, T. A., Meshcheryakova, E. N., & Tulchinsky, V. M. (1974) *Int. J. Pept. Protein Res.* **6**, 465.  
 Popov, E. M., Pletnev, V. Z., Evstratov, A. V., Ivanov, V. T., & Ovchinnikov, Y. A. (1970) *Khim. Priir. Soedin.*, 616.  
 Shanzer, A., Felder, C. E., & Lifson, S. (1983) *Biopolymers* **22**, 409.  
 Tishchenko, G. N., Karimov, Z., Vainshtein, B. K., Evstratov, A. V., Ivanov, V. T., & Ovchinnikov, Y. A. (1976) *FEBS Lett.* **65**, 315.  
 Tishchenko, G. N., Karaulov, A. I., & Karimov, Z. (1982) *Cryst. Struct. Commun.* **11**, 451.  
 Warshel, A. (1981) *Acc. Chem. Res.* **14**, 284.

## Cytochromes *c'* in Their Reaction with Ethyl Isocyanide<sup>†</sup>

Steven C. Rubinow and Richard J. Kassner\*

**ABSTRACT:** The binding of ethyl isocyanide (EIC) to a representative number of cytochromes *c'* is demonstrated. Spectroscopic and equilibrium constants have been measured and compared for the binding of EIC to cytochromes *c'* from the photosynthetic bacteria *Chromatium vinosum*, *Rhodospseudomonas palustris*, *Rhodospirillum rubrum*, and *Rhodospseudomonas sphaeroides*. While the absorption spectra of the EIC complexes resemble those of EIC complexes of other high-spin hemoproteins, the Soret half band widths and extinction coefficients per heme exhibit more than a 2-fold difference with the values of *C. vinosum* being most similar to those of *Rh. sphaeroides* and of *Rh. palustris* similar to those of *Rs. rubrum*. The cytochromes exhibit binding equilibria consistent with the ligation of one molecule of EIC per heme in contrast to the reported binding of more than one molecule of CO per heme. The binding constants exhibit more than a 1000-fold difference with the values of *C. vinosum* being

closely similar to those of *Rh. sphaeroides* and of *Rh. palustris* similar to those of *Rs. rubrum*. The lack of correlation between EIC and CO binding properties indicates that electronic factors do not determine the difference in EIC binding properties. The observed correlation between the extinction coefficients, half band widths, and equilibrium constants for EIC complex formation provides the first spectroscopic evidence that the differences in binding properties are associated with sterically hindered ligation to the heme. Although the differences in binding properties provide evidence of steric hindrance, the EIC binding constants for particular cytochromes *c'* indicate that the distal heme binding site is more accessible than previously indicated. The differences in spectroscopic and binding properties are discussed in terms of structural differences between amino acids thought to be associated with the distal heme binding site.

**T**he cytochromes *c'* are mono- and diheme proteins derived from photosynthetic and denitrifying bacteria and are reported

to comprise the largest and most widespread class of bacterial cytochromes known (Meyer & Kamen, 1982). These cytochromes are thought to function in electron transport although no specific role has been ascribed to them (Bartsch, 1978). The proteins have been found to exhibit properties similar to functionally different classes of hemoproteins. The cyto-

<sup>†</sup> From the Department of Chemistry, University of Illinois at Chicago, Chicago, Illinois 60680. Received September 19, 1983. This investigation was supported by grants from the National Institutes of Health (AM 28188 and HL 26216).